Steel and Composite Structures, *Vol. 28, No. 2 (2018) 167-177*
DOI: https://doi.org/10.12989/scs.2018.28.2.167

Experimental and theoretical studies on SHS column connection with external stiffening ring under static tension load

Bin Rong [1,2a], Guangchao You [1b], Ruoyu Zhang [*1], Xu Ma [1] and Xinxin Quan [1]

[1] *Department of Civil Engineering, Tianjin University, Tianjin, 300072, China*
[2] *Key Laboratory of Coast Civil Structure Safety, Tianjin University, Tianjin, 300072, China*

(*Received July 29, 2017, Revised February 2, 2018, Accepted May 24, 2018*)

Abstract. In order to investigate mechanical properties in the core area of Square Hollow Section(SHS) column connection with external stiffening ring, four specimens were tested under the static tension load. The failure modes, load-displacement curves and strain distribution were analyzed to study the mechanical properties and the load transfer mechanism of the core area of connections. The connections behave good ductility and load-bearing capacity under the static tension load. Parametric analysis was also conducted, in which the thickness of steel tube, extended width and thickness of the stiffening ring were considered as the parameters to investigate the effects on mechanical properties of the connections. Based on the experimental results, an analytical method for the bearing capacity of connection with external stiffening ring under the static tension load was proposed. The theoretical results and the experimental results are in good agreement, which indicates that the theoretical calculation method of the bearing capacity is advisable.

Keywords: connection with external stiffening ring; static tensile loading experiment; failure mode; parametric analysis; strain distribution; bearing capacity

1. Introduction

Connection is the most important part of the steel frame structure. It not only plays the role of transferring load and distributing internal force in the structural system, but also ensures the integrity of the structure. At present, domestic and foreign scholars have proposed a variety of connection between rectangular steel tube column and H-shaped steel beam, such as Internal Diaphragm Connection, Through-Diaphragm Connection and Connection with External Stiffening Ring, as shown in Fig. 1.

Connection with external stiffening ring between square steel tube column and H-shaped steel beam has gained a widespread usage in composite frame structures because of its good bearing capacity, ductility, seismic-resisting and constructional convenience. What's more, the steel tube column of the connection with external stiffening ring is not cut off in the manufacture which ensures the integrity of the steel tube column and makes the construction more convenient than the other two connections.

In the past, a large amount of researches have been conducted on the connections between square steel tubular column and H-shaped steel beam. The structural behavior of internal-diaphragm connections between Concrete-Filled Rectangular Tubular column (CFRT column) and steel beam has been studied by Sasaki *et al.* (1995), Zhou *et al.* (2005) and Park *et al.* (2010). An analytical model for the flexural capacity of internal-diaphragm connections with anchored studs was proposed by Nie *et al.* (2009). Lu *et al.* (2000) tested five interior diaphragm connections and found that the flexural bearing capacity of the panel zone should take into account the contribution of the interior diaphragm and the steel tube while the contribution of concrete is small and can be neglected. Based on finite element modes of internal diaphragm connection and through-diaphragm connection set up by Yu *et al.* (2015), the out-of-plane deformation at column flange, force flow pattern and shear and moment transfer efficiency of WF (Wide Flange) - beam to rectangular CFT (Concrete-Filled Tube) column connection were discussed, and the results show that both poisson effect and flexibility of column flange will lead to a change on force flow pattern in beam–column junction region and inefficient moment transferring ability through beam web, resulting in a high level of hydrostatic stress demand at beam flanges. Lee *et al.* (2011) analyzed the stress distribution regularity of ring plate of CFST (Concrete Filled Steel Tubular) connections with exterior diaphragms. Chiew *et al.* (2001) investigated the moment resistance of steel I-beam to concrete-filled Steel tube column uniplanar connections under monotonic static loading and derived an empirical formula based on numerical parametric analysis results. Two analytical models were established to predict the shear stiffness and yield shear strength of the hollow structural sections beam and panel zone by Qin *et al.* (2014a, b). Theoretical study on the seismic behavior of the connections between CFRT (Concrete-Filled Rectangular Tube) columns and steel H-beams has been conducted by Fukumoto and Morita (2005),

∗Corresponding author, Ph.D.,
E-mail: zryu@163.com
[a] Ph.D., E-mail: tjerobin@126.com
[b] E-mail: youguangchao@163.com

ISSN: 1229-9367 (Print), 1598-6233 (Online)

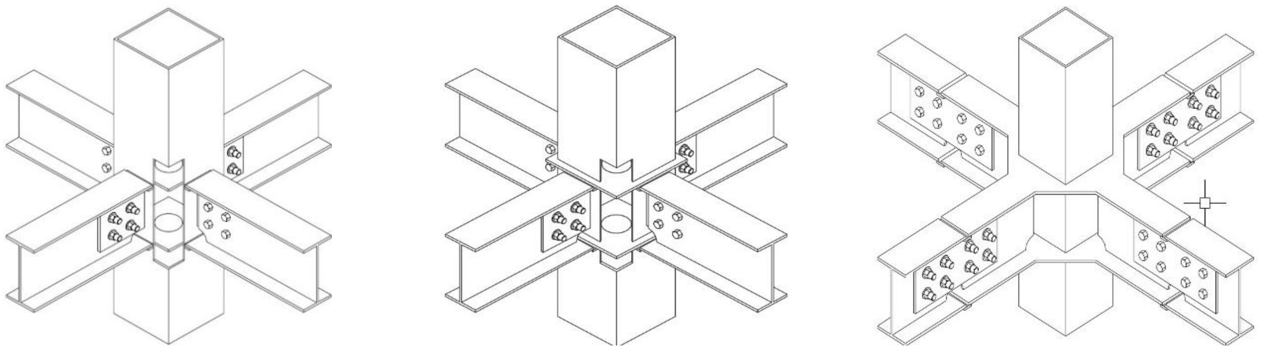

(a) Internal diaphragm connection (b) Through-diaphragm connection (c) Connection with external stiffening ring

Fig. 1 Connections between rectangular steel tube column and H-shaped steel beam

Qin *et al*. (2014a, b), Choi *et al*. (2010), Han and Li (2010), Han *et al*. 2008), Guo and Yao (2012). Static tensile loading experiments and nonlinear finite element analysis were carried out to study the mechanical properties and failure modes of through-diaphragm joints of concrete-filled square steel tubular columns by Rong *et al*. (2013). Five experimental specimens were carried out and a finite element analysis is presented to model the non-linear behavior of the in-plane moment connections between steel I-beams and square steel tube columns with stiffening plates around the columns under vertical loads only by Dessouki *et al*. (2015).

At present, the investigations are mainly focused on the seismic behavior of the through-diaphragm connections and internal-diaphragm connection between concrete-filled square steel tubular columns and steel beam. However, few studies have considered the performance in the core area of the connection with external stiffening rings between SHS columns and steel beams under bending moment. Connections with external stiffening rings between SHS columns and steel beam has been widely used in steel frame structures because of the benefits of excellent mechanical behavior and architecturally pleasing advantages (Qin *et al*. 2014c). However, because of the lack of design guidance and a unified method for calculating the bearing capacity of the connection, the use of connection with external stiffening rings is limited. Therefore, it is necessary to investigate the mechanical property of connections with external stiffening rings systematically considering those factors.

In this paper, four specimens were tested under static tension load to investigate the mechanical properties and load-bearing capacity in the core area of SHS column connection with external stiffening ring. Specimens failure modes, load-displacement curves and strain distribution were studied to analyze the mechanical properties and the load transferring mechanism of the specimens.

2. Experimental program

2.1 Test specimens

As we all know, the beam is bent and deformed under the action of vertical load. It results in the upper flange of the beam being pulled and the lower flange of the beam be compressed. If the height of beam is H, the tension of the upper flange is F. The connections with external stiffening rings are designed according to the assumption that the bending bearing capacity of the connection can be obtained by multiplying the tensile bearing capacity of the connection domain (F) and the distance between the tensile load and the center of curvature of the separator resistance (H) (Morino and Tsuda 2002). Thickness of steel tube t_c,

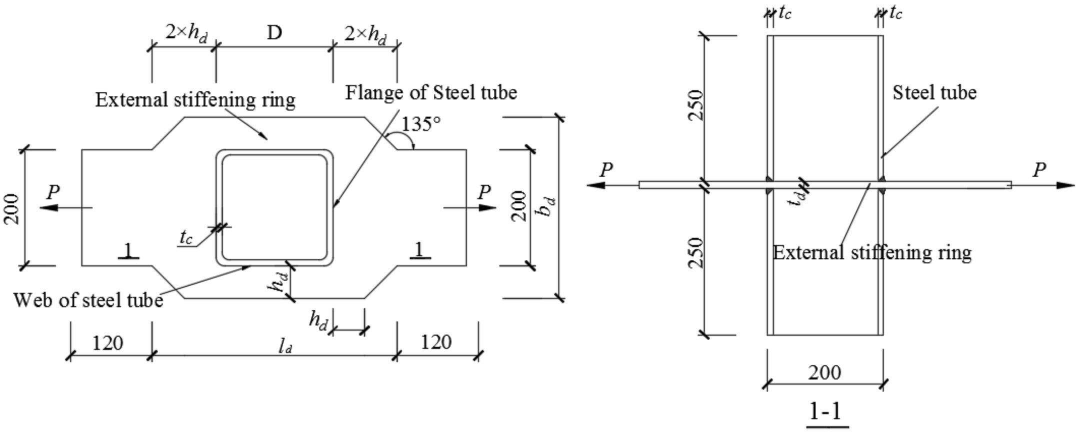

Fig. 2 Configuration of specimens

Table 1 Dimensions of specimens

Specimens	Steel tubes	External stiffening rings			
	$D \times t_c$ (mm)	h_d	b_d	t_d	l_d
TS1	200×6	40	280	12	360
TS2	200×6	60	320	12	440
TS3	200×8	40	280	12	360
TS4	*200× 6*	*40*	*280*	*10*	*360*

extended width h_d and thickness of the stiffening ring t_d were considered as the parameters to investigate the effects on the bearing capacity of the connections under the static tension load. Four specimens of connections with external stiffening rings were designed for the static tensile test, as shown in Fig. 2. A scale factor of 1⁄2 was chosen considering the loading capacity and the size of the testing apparatus. The height of the column was 500 mm. The dimension of all steel tubes was 200 mm × 200 mm. The external stiffening rings are cut into a whole plate and connected with the steel column by butt weld. Detailed dimensions of each specimen are listed in Table 1. The flange of the steel tube and the web of the steel tube are respectively the planes of the steel tube indicated in the Fig. 2.

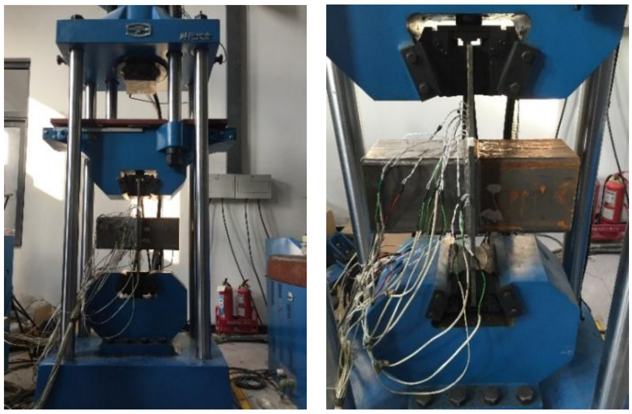

Fig. 3 Loading set-up

2.2 Material properties

Three tensile coupons for each thickness were cut from steel tubes and steel plates. They were tested by the same test conditions to obtain the modulus of elasticity (E_S), the yield strength (f_y), the ultimate strength (f_u), the yield ratio (f_y/f_u), and the elongation ratio δ. Material properties for the steel are shown in Table 2.

Table 2 Material properties of steel

Component	Thickness (mm)		f_y (N/mm^2)	f_u (N/mm^2)	E_s (10^{5}N/mm^2)	δ (%)
Steel tube	6	5.68	308.7	443.9	2.036	33.6
	8	7.89	278.1	409.3	2.180	38.7
Steel plate	10	9.62	302.5	421.4	2.044	37.4
	12	11.48	273.8	429.8	2.167	34.6

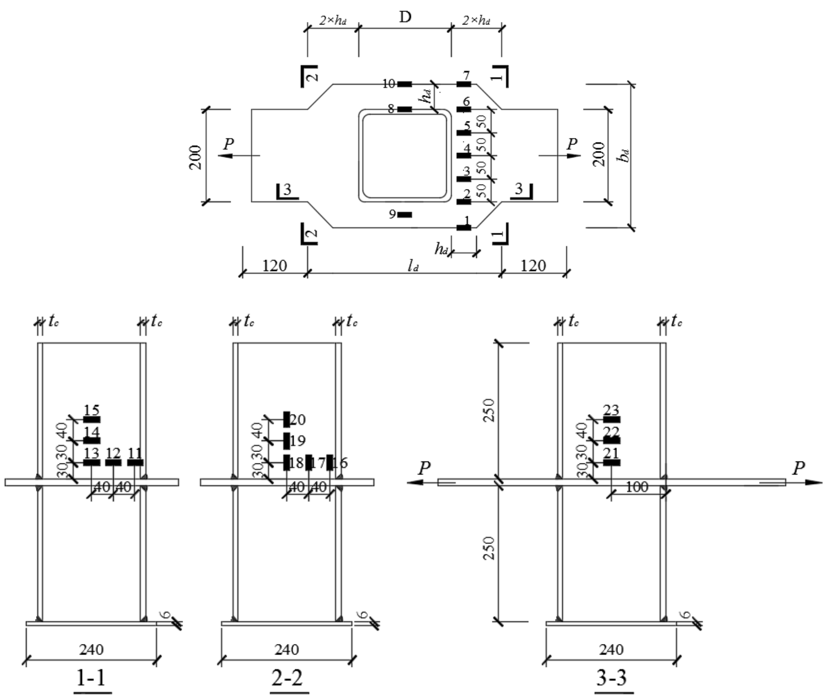

Fig. 4 Layout of strain gauges

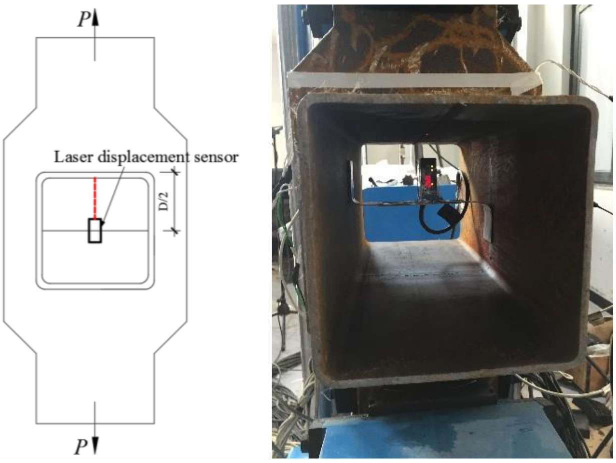

Fig. 5 Layout of laser displacement sensor

2.3 Test setup and loading

Controlled Electro-Hydraulic Servo Universal Testing machine was used to the static tensile test. The loads were applied on the beam flanges of both sides of the column until the failure occurred. Before the test, the specimens were preload in order to ensure the normal operation of each part of the test. Monotonic loading method was adopted in the experiment. Loading scheme was controlled by the load in the elastic range, and each load increment was 1/10 of the estimated ultimate load. Each load interval was maintained for about 3~5 minutes. Once the connections yield, loading scheme would be controlled by displacement, and the displacement speed was 1 mm/min.

2.4 Measuring-point arrangement

Fig. 4 shows the layout of strain gauges. Twenty-three strain gauges were arranged in specimens TS1 and TS2 to analyze the stress distribution of connections during loading process. The values of strain gauges were collected automatically by the highly speed data acquisition system. The tensile displacements of the stiffening rings were measured automatically by the testing machine. In addition, in order to study the deformation of steel tube column flange, a laser displacement sensor was installed in the center of the steel tube as shown in Fig. 5.

2.5 Test results and discussion

2.5.1 Experimental phenomena

Failure modes of the specimens were shown in Fig. 6. According to the phenomena of the test specimens, there are three kinds of failure modes of connections with external stiffening rings.

(1) Bending failure in the column flanges

During the early stage of loading, no cracks were observed on concrete surface and there were no obvious deformations in the steel tube column of specimen TS1. With the increase of loading, the connection began to yield and the deformation increased rapidly. As shown in Fig. 6(a), there was necking phenomena in the chamfering position of the stiffening ring. When the load reached the failure load, the flanges of steel tube column were obviously swelled under tensile load and the webs of the steel tube column have an inward depression. There was no obvious crack in specimen TS1 during the whole loading process. In the end, the specimen TS1 failed, owing to steel tube bending in the column flanges and large deformation. The maximum deformation of the steel tube flanges is 14.6 mm measured by the laser displacement sensor.

(2) Weld failure

At the initial stage of loading, the phenomena of the specimen TS2 is similar to that of the specimen TS1. With the increase of the load, the connection began to yield and the deformation increased. As shown in Fig. 6(b), when the load reached the maximum, the weld between the stiffening ring and steel tube column cracked abruptly. The bearing capacity began to decline and the displacement increased rapidly. With the increase of the displacement and the expansion of the crack, the stiffening ring began to fail. In the end, the specimen TS2 failed, owing to the failure of weld in the core area of the connection.

(3) Stiffening ring failure

The specimen TS3 and the specimen TS4 failed at the chamfering position of the stiffening ring. At the initial stage of loading, there were no significant changes in the whole specimen, as shown in Fig. 6(b)-(c). With the increase of the load, there was necking phenomena in the chamfering position of the stiffening ring and the displacement increased rapidly. In the end, the specimen TS3 and TS4 failed, owing to stiffening ring break. Compared with the specimens TS1 and TS2, there was no obvious deformation in the core area of connections during the whole loading process.

2.5.2 Load-displacement curves

Fig. 7 shows the load-displacement curves of the specimens. All curves exhibit elastic behavior at the initial stage followed by an extensive plastic until failure plateau. Combining the failure mode and the load-displacement curve shape of each specimen, it can be found that TS3 and TS4 failed abruptly, and the load drops suddenly after reaching the ultimate load. The failure mode of TS2 is weld failure. It can be seen that the load-displacement curves decreased slowly after the weld damage. What is more, there is a large deformation after destruction. It indicates that the specimen TS2 is not completely failure and can continue to work and this kind of connection has good ductility. The failure mode of TS1 is bending failure in the column flanges. Its load-displacement curve is relatively smooth, and there is no sudden drop. All the curves are in good agreement with the experimental phenomena. The deformation of specimen TS4 is smaller than that of other specimens, which is due to that the small thickness of the stiffening ring cannot give full play to the deformation capacity of the steel tube.

The yield load p_y^e and the ultimate load p_u^e which are obtained from the load-displacement curve of each

(a) TS1

(b) TS2

(c) TS3

(d) TS4

Fig. 6 Failure modes

specimen are listed in Table 3. The ultimate load p_u^e is defined as the maximal load of the connection. The yield load p_y^e is obtained by a graphical method (Nie *et al*. 2008). Δ is the maximum deformation of the steel tube

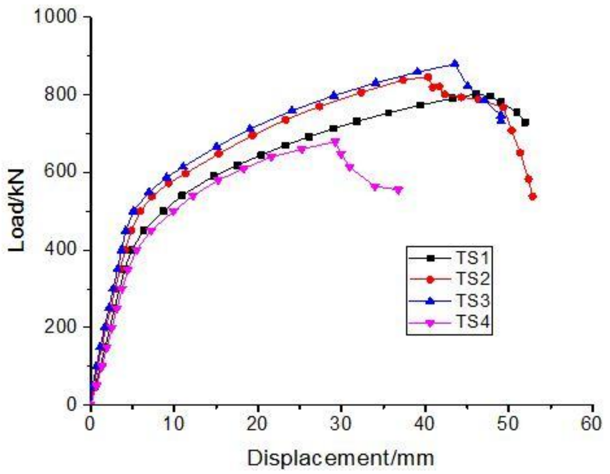

Fig. 7 Load-displacement curves

Table 3 Bearing capacity of specimens

Specimens	p_y^e (kN)	p_u^e (kN)	Δ (mm)
TS1	506.1	801.7	14.6
TS2	566.5	866.6	10.9
TS3	587.9	879.6	12.7
TS4	455.8	660.8	9.4

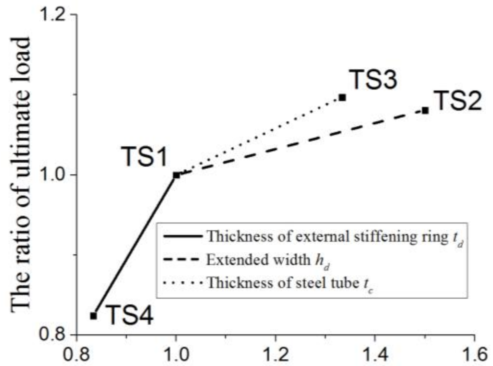

Fig. 8 Non-dimensional analysis

measured by the laser displacement sensor.

2.5.3 Parametric analysis

In this study, factors that were taken into discussion include: thickness of steel tube t_c, extended width h_d and thickness of the stiffening ring t_d. A parametric study was conducted based on the experimental results. Fig. 8 shows the result of the non-dimensional parametric analysis. The vertical axis is the ratio of ultimate load of other specimens to ultimate load of TS1. For the specimen TS2, the horizontal axis is the ratio of the extended width of the stiffening ring of TS2 to the extended width of the stiffening ring of TS1. For the specimen TS3, the horizontal axis is the ratio of the thickness of steel tube of TS3 to the thickness of steel tube of TS1. For the specimen TS4, the horizontal axis is the ratio of the thickness of the stiffening ring of TS4 to the thickness of the stiffening ring of TS1.

(1) Extended width of the stiffening ring

For specimens TS1 and TS2, the dimensions and material properties are the same except for the extended width of the stiffening ring h_d, which is 40 mm for TS1 and 60 mm for TS2. Comparing the load-displacement curves TS1 with TS2 in Fig. 7 and the result of the non-dimensional parametric analysis in Fig. 8. The extended width of the stiffening ring increases It shows that the width of the stiffening ring has a contribution to improve the bearing capacity of the connection.

(2) Thickness of steel tube

For specimens TS1 and TS3, the dimensions and material properties are the same except for the thickness of steel tube t_c, which is 6 mm for specimen TS1 and 8 mm for specimen TS3. Comparing the load-displacement curves of TS1 and TS3 in Fig. 7, their ultimate load in Table 4 and the result of the non-dimensional parametric analysis in Fig. 8. The thickness of steel tube increases by 1.333 times and the ultimate load increases by 1.097 times. The ultimate load increases from 801.7 kN for TS1 to 879.6 kN for TS3. It shows that the effect of the thickness of steel tube is significant for improving the bearing capacity of the connection. The stiffness of steel tube increased with the increase of thickness of steel tube. It avoids the bending failure in the column flanges and improves the bearing capacity of the connection.

(3) Thickness of the stiffening ring

For specimens TS1 and TS4, the dimensions and material properties are the same except for the thickness of the stiffening ring t_d, which is 12 mm for specimen TS1 and 10 mm for TS4. Comparing the load-displacement curves of TS1 and TS4 in Fig. 7 and the result of the non-dimensional parametric analysis in Fig. 8. The thickness of steel tube decreases by 0.833 times and the ultimate load decreases by 0.824 times. It can be seen that the effect of the thickness of steel tube on improving the bearing capacity is most obvious. It is apparent that the larger thickness of the stiffening ring is beneficiary leading to larger failure load and larger deformation at the failure point. Note that the increase of the thickness of the stiffening ring has a little effect on the stiffness of the specimens.

2.5.4 Strain distribution

A large number of strain gauges were arranged on specimens TS1 and TS2 to observe the strain distribution of the connections in the whole loading process. Analyzing the test data can obtain the stress distribution of the connections and help to study the stress transferring mechanism and failure mechanism of the core area of the connections under static tensile load. It provides the experimental basis for the research on the calculation of the bearing capacity of the core area of the connections. Figs. 9(a) and (b) shows the strain distribution of strain gauges 1-7 under different load levels. The horizontal axis is the number of the strain gauges, and the vertical axis is the strain value. The overall characteristics of the strain distribution of the two specimens are consistent. It can be seen that the stress distribution is not uniform in the whole loading process.

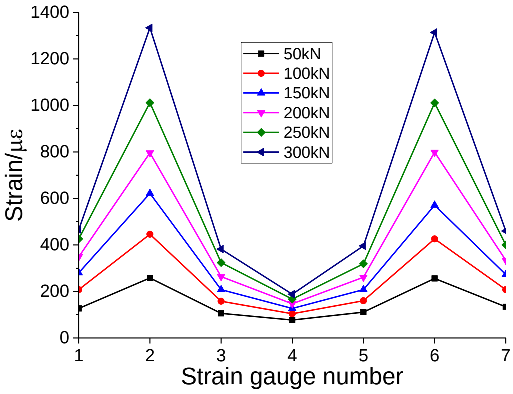

(a) TS1

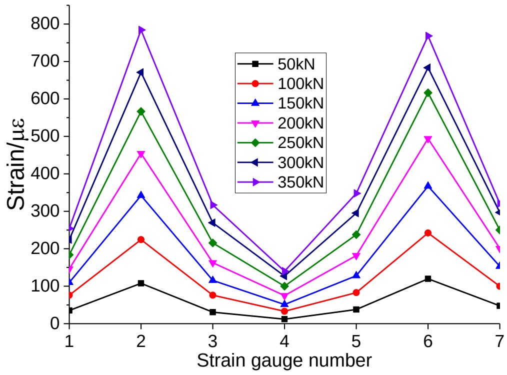

(b) TS2

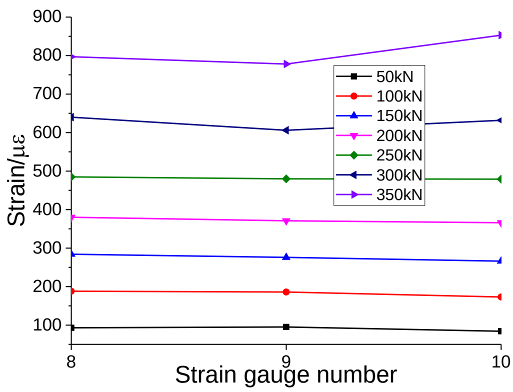

(c) TS1

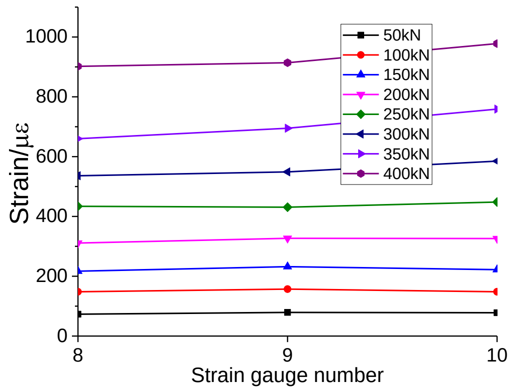

(d) TS2

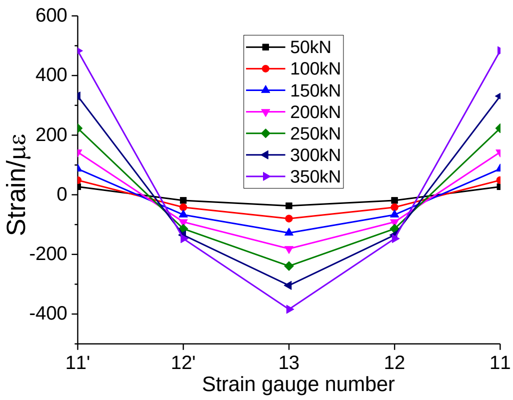

(e) TS1

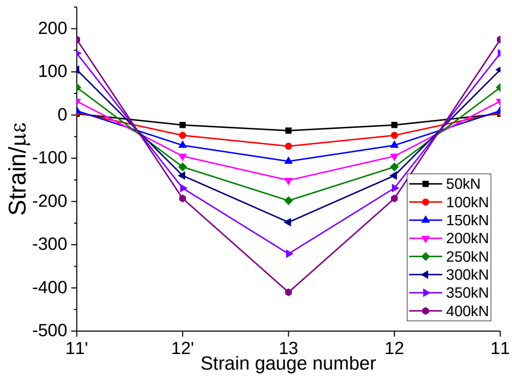

(f) TS2

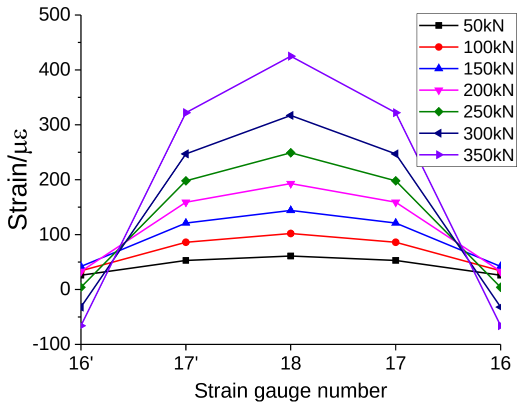

(g) TS1

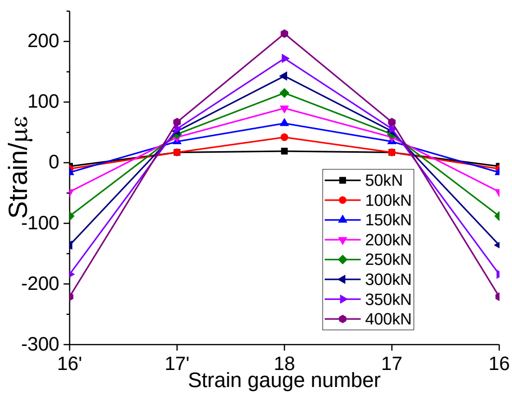

(h) TS2

Fig. 9 Distribution of strain gauge

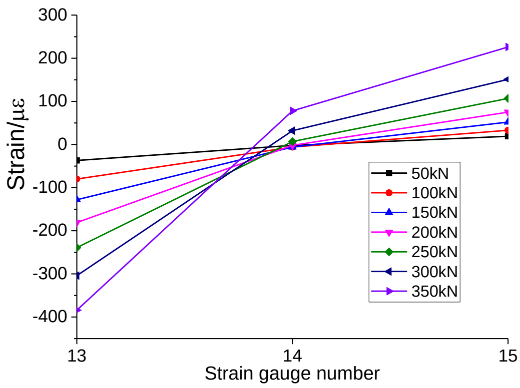

(i)TS1

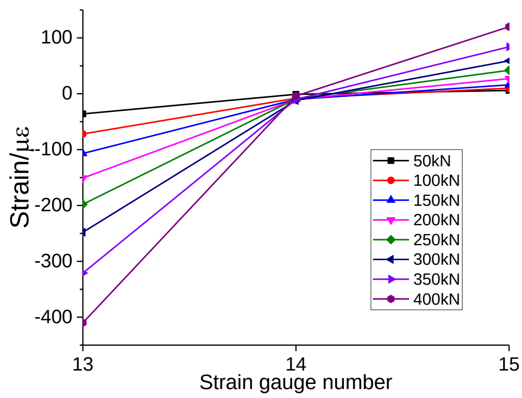

(j)TS2

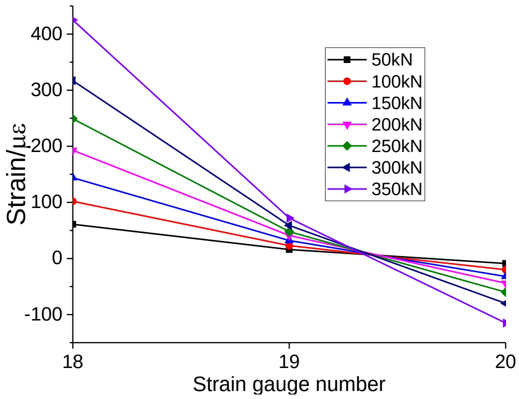

(k)TS1

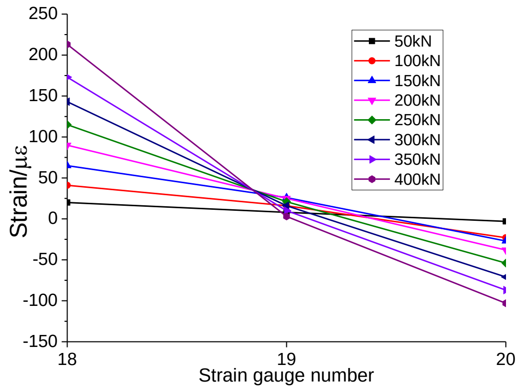

(l)TS2

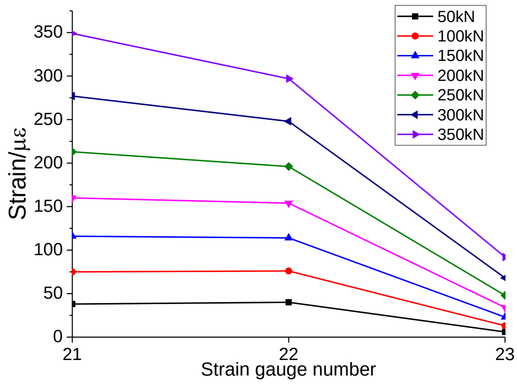

(m)TS1

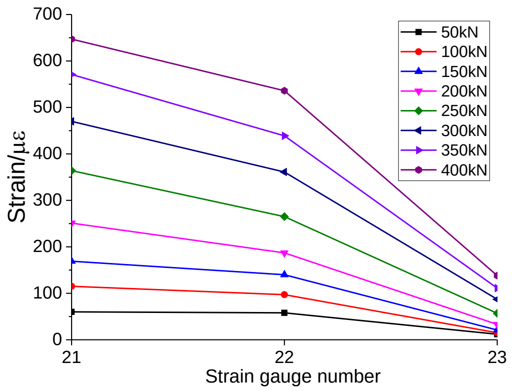

(n)TS2

Fig. 9 Continued

The stress in the middle and the edge of the stiffening ring is small, column is large. With the increase of the load, the stress non-uniformity becomes more and more obvious. The stress distribution of strain gauge 1-7 is M-shaped. The reason is that the stiffness of the column flanges is weak, and the stress mainly transmitted through the column webs and the stiffening ring. Comparing the strain of the specimen TS1 and TS2, it can be found that the strains of specimen TS1 are obviously larger than those of specimen TS2 under the same load level. It indicates that increasing the width of the stiffening ring is of great benefit to the diffusion of the load.

Figs. 9(c) and (d) shows the strain distribution of strain gauges 8-10 under different load levels. It can be found that the stress level of the stiffening ring is very high, which indicates that overhanging part of the stiffening ring bears the most majority of the tensile load. The strain distribution is uniform in the whole loading process. Therefore, it is reasonable to assume that the stress distributed uniformly on the overhanging part of the stiffening ring when calculating the bearing capacity of the stiffening ring. At the initial stage of loading, the strain grows slowly. With the increase of the load level, the strain growth rate is accelerated. It shows that the stiffness of the specimen is large in the elastic stage and the stiffness of the connection decreased after yielding. Comparing the strain of specimen

TS1 and specimen TS2, it can be seen that with the increase of extended width of the stiffening ring, the strain of specimen TS1 are obviously larger than those of specimen TS2 under the same load level.

Figs. 9(e), (f), (g) and (h) show the strain distribution of strain gauges 11-13 and 16-18 under different load levels. At the initial stage of loading, the strain distribution is uniform. With the increase of the load, the strain difference of each point gets larger. From point 11 to point 13 (or point 17 to 18), the strain value changed from negative to positive. It can be seen that the stress near the point 13 and 12 (or 18 and 17) is mainly along the axis of the column. On the contrary, the stress near the point 11 (or 16) is perpendicular to the axis of the column. It indicates that the flange of steel tube column was obviously swelled under tensile load and the load on the flange of steel tube column is transferred to the web of steel tube column finally.

Figs. 9(i), (j), (k) and (l) show the strain distribution of strain gauges 13-15 and 18-20 under different load levels. Respectively, strain gauges 13-15 and strain gauges 18-20 are arranged in the same position, but the direction is different. With the increase of the height, the stress decreases gradually. Stress concentration appears near the stiffening ring. The stress level in the region far from the stiffening ring is low. From point 13 to15 (or 20 to 18), the strain value changed from negative to positive, which means that the steel tube flange in the vicinity of the point 15 (or point 20) is in a state of transverse tension. It indicates that the stress on the steel tube column flange is transferred from the column flange to the two webs rather than along the axis of the column.

Figs. 9(m) and (n) shows the strain distribution of strain gauges 21-23 under different load level. It can be seen that the stress decreases rapidly with the increase of the height.

With the increase of the load, the stress of the steel tube column near the stiffening ring increases rapidly. However, there is little change in stress of the area away from the stiffening ring. It shows that the height of the steel tube column web bearing the tensile load is limited. Therefore, the effective height of the steel tube column web wall should be considered in the calculation of bearing capacity. It can be found that the strain of specimen TS1 is obviously larger than that of specimen TS2 in the same loading level, because the extended width of the stiffening ring of specimen TS2 is larger than that of the specimen TS1. It shows that increasing the width of the stiffening ring can effectively improve the bearing capacity of the connection.

3. Theoretical analysis

According to the analysis of experimental results, the analytical method for calculation of the bearing capacity of the core area of the connections is proposed.

3.1 Load transfer mechanism

Under tensile loading, the stiffening ring is extended along the stress direction and the webs of steel tube column were obviously swelled. When the specimens were failed, the stress level of the overhanging section of the stiffening ring is very high and the yield region of steel tube column is mainly concentrated around the stiffening ring. The results of parametric analysis show that the bearing capacity of the connections is related to the thickness of steel tube, extended width of the stiffening ring and the thickness of the stiffening ring. According to the experimental observations and stress mechanism, it can be found that the

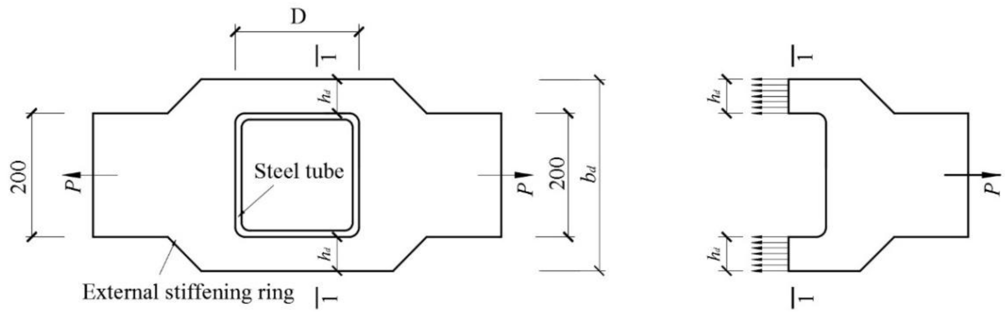

(a) Calculation model of the stiffening ring

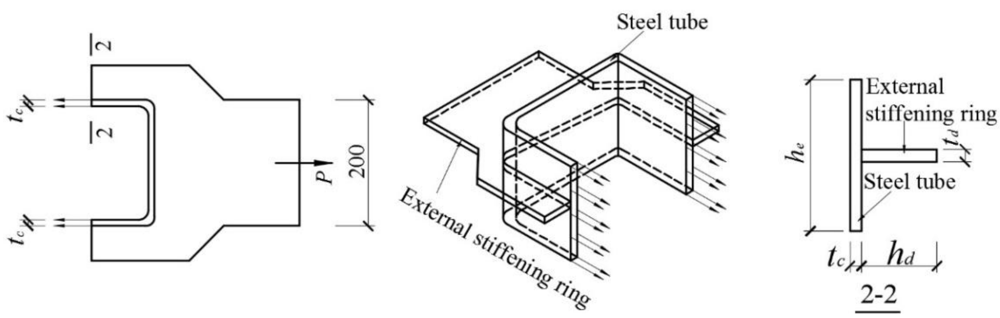

(b) Calculation model of the steel tube

Fig. 10 Calculation model

Table 4 Comparison of bearing capacity

Specimen	Yield bearing capacity			Ultimate bearing capacity		
	p_y^e (kN)	p_y (kN)	p_y/p_y^e	p_u^e (kN)	p_u (kN)	p_u/p_u^e
TS1	506.1	495.1	0.97	801.7	745.4	0.93
TS2	566.5	620.4	1.09	866.6	942.4	1.09
TS3	587.9	625.6	1.06	879.6	928.3	1.06
TS4	455.8	470.3	1.05	679.8	666.3	1.01

horizontal load transferred from the steel beam flange is borne by the two parts. One part is directly transferred to the stiffening ring, and the other part is transferred to the steel tube column through the stiffening ring.

3.1.1 Load transfer mechanism of the stiffening ring

According to the failure characteristics of the stiffening ring in specimen TS2, it can be found that the stiffening ring destroyed for it reached the limit of bearing capacity. As shown in Fig. 10(a), assuming that the stress in the ring plate overhanging section is evenly distributed, and the 1-1 section is the weakest section based on the analytical results of strain distribution. According to the static equilibrium theory, the bearing capacity of the stiffening ring can be expressed as Eq. (1).

$$p_{y1}^d = 2h_d t_d f_y^d \tag{1}$$

Where, t_d is the thickness of the stiffening ring, f_y^d is the yield strength of stiffening ring and h_d is extended width of the stiffening ring.

3.1.2 The yield mechanism of the steel tube

According to the results of strain analysis, under tensile load and the load on the flange of steel tube column is transferred to the web steel tube column finally. When the specimens were failed, the webs of steel tube column were obviously swelled. The effective height h_e of the steel tube column web should be considered in the calculation of the bearing capacity. Fig. 10(b) shows the calculation model of steel tube column.

Based on the theory of elastic foundation beam, the effective height h_e of the steel tube column web is derived by Zhong (2003).

$$h_e = \left(0.63 + 0.88\frac{b_f}{d}\right)\sqrt{dt} + t_d \tag{2}$$

Where, b_f is the width of the beam flange, $d = 2D/\sqrt{\pi}$ is the equivalent circle diameter. $t = 2t_c/\sqrt{\pi}$ is the equivalent circle thickness. D is the width of the steel tube column. t_c is the thickness of the steel tube column. t_d is the thickness of the stiffening ring.

Put the equivalent circle diameter and thickness into Eq. (2)

$$h_e = \left(0.63 + 0.88\frac{b_f}{d}\right)\sqrt{dt} + t_d = 1.7951\sqrt{Dt_c} + t_d \tag{3}$$

The total contribution from the steel tube column can be expressed as Eq. (4).

$$p_y^c = 2h_e t_c f_y^c \tag{4}$$

3.2 Verification of the analytical method

The calculation formula of bearing capacity of connections with the stiffening ring can be obtained by superposition of the bearing capacity of the stiffening ring and the steel tube web

$$p_y = p_y^d + p_y^c \tag{5}$$

In order to validate the accuracy of the analytical method proposed above, the experimental yield p_y^e and ultimate bearing capacity p_u^e of static tensile loading tests are compared with the calculated ones, as shown in Table 4. The ultimate bearing capacity p_u of the specimens, can be calculated by using Eq. (5) if the yield strength f_y^d and f_y^c are substituted by the ultimate strength f_u^d and f_u^c.

Comparisons of the experimental and theoretical values for yield and ultimate bearing capacity shown in Table 4. It can be seen that the theoretical calculation results consist well with the ultimate bearing capacity measured by the static tensile test. Specimen TS3 and TS4 failed in the chamfering position of the stiffening ring and specimen TS2 failed because the weld between the stiffening ring and steel tube column cracked abruptly. Therefore, the observed ultimate strength is smaller than the calculated values. It shows that the theoretical calculation method of the bearing capacity is advisable.

4. Conclusions

Four specimens were tested under static tension load to investigate mechanical properties and load-bearing capacity of SHS column connection with external stiffening ring. Based on the experimental results, the calculation formula for the bearing capacity of connection with external stiffening ring under static tension load was proposed. The main conclusions can be summarized as follows:

- The experimental results show that there are three kinds of failure modes of connections with external stiffening rings, including bending failure in the column flanges, weld failure and stiffening ring failure. All specimens show goodductility and load-bearing capacity.

- According to the results of the parametric analysis, thickness of steel tube, extended width and thickness of the stiffening ring all have significant effect on the bearing capacity of the connection.
- Strain distribution results show the flange of steel tube column was obviously swelled under tensile load and the load on the flange of steel tube column is transferred to the web steel tube column finally. Increasing the width of the stiffening ring can share the load of steel tube column and effectively improve the bearing capacity of the connection.
- According to the experimental observations and stress mechanism, it can be considered that the horizontal load transferred from the steel beam flange is borne by two parts. One part is directly transferred to the stiffening ring, and the other part is transferred to the steel tube column through the stiffening ring.
- Results of theoretical calculation and static tension experiment accord well with each other. It shows that the theoretical calculation method of the bearing capacity is advisable.

Acknowledgments

The research described in this paper was financially supported by the National Natural Science Foundations of China (No. 51468061, No. 51268054 and No. 51468061) and the Natural Science Foundation of Tianjin City, China (No. 13JCQNJC07300). The financial supports are greatly appreciated.

References

Chiew, S.P., Lie, S.T. and Dai, C.W. (2001), “Moment resistance of steel I-beam to CFT column connections”, *J. Struct. Eng.*, **127**(10), 1164-1172.

Choi, S.M., Park, S.H., Yun, Y.S. and Kim, J.H. (2010), “A study on the seismic performance of concrete-filled square steel tube column-to-beam connections reinforced with asymmetric lower diaphragms”, *J. Constr. Steel Res.*, **66**(7), 962-970.

Dessouki, A.K., Yousef, A.H. and Fawzy, M.M. (2015), “Investigation of in-plane moment connections of I-beams to square concrete-filled steel tube columns under gravity loads”, *Hbrc Journal*, **11**(1), 43-56.

Fukumoto, T. and Morita, K. (2005), “Elastoplastic behavior of panel zone in steel beam-to-concrete filled steel tube column moment connections”, *J. Struct. Eng.*, **131**(12), 1841-1853.

Guo, Y. and Yao, X. (2012), “Seismic performance and design of reduced steel beam section with concrete filled square tubular column”, *Adv. Steel Constr.*, **9**(3), 173-189.

Han, L.H. and Li, W. (2010), “Seismic performance of CFST column to steel beam joint with RC slab: Experiments”, *J. Constr. Steel Res.*, **66**(11), 1374-1386.

Han, L.H., Wang, W.D. and Zhao, X.L. (2008), “Behaviour of steel beam to concrete-filled SHS column frames: finite element model and verifications”, *Eng. Struct.*, **30**(6), 1647-1658.

Lee, C.Y., Luo, L. and Guo, Y.J. (2011), “Stress distribution regularity analysis of ring plate of concrete filled steel tube connections with exterior diaphragms”, *Adv. Mater. Res.*, **163-167**, 1945-1950.

Lu, X., Yu, Y., Kiyoshi, T. and Satoshi, S. (2000), “Experimental study on the seismic behavior in the connection between CFRT column and steel beam”, *Struct. Eng. Mech., Int. J.*, **9**(4), 365-374.

Morino, S. and Tsuda, K. (2002), “Design and construction of concrete-filled steel tube column system in Japan”, *Earthq. Eng. Eng. Seismol.*, **4**(1), 51-73.

Nie, J., Qin, K. and Cai, C.S. (2008), “Seismic behavior of connections composed of CFSSTCs and steel–concrete composite beams-experimental study”, *J. Constr. Steel Res.*, **64**(10), 1178-1191.

Nie, J.G., Qin, K. and Cai, C.S. (2009), “Seismic behavior of composite connections-flexural capacity analysis”, *J. Constr. Steel Res.*, **65**(5), 1112-1120.

Park, S.H., Choi, S.M., Kim, Y.S., Park, Y.W. and Kim, J.H. (2010), “Hysteresis behavior of concrete filled square steel tube column-to-beam partially restrained composite connections”, *J. Constr. Steel Res.*, **66**(7), 943-953.

Qin, Y., Chen, Z. and Wang, X. (2014a), “Elastoplastic behavior of through-diaphragm connections to concrete-filled rectangular steel tubular columns”, *J. Constr. Steel Res.*, **93**(1), 88-96.

Qin, Y., Chen, Z. and Han, N. (2014b), “Research on design of through-diaphragm connections between CFRT columns and HSS beams”, *Int. J. Steel Struct.*, **14**(3), 589-600.

Qin, Y., Chen, Z., Wang, X. and Zhou, T. (2014c), “Seismic behavior of through-diaphragm connections between CFRT columns and steel beams-experimental study”, *Adv. Steel Constr.*, **10**(3), 351-371.

Rong, B., Chen, Z., Zhang, R., Fafitis, A. and Yang, N. (2013), “Experimental and analytical investigation of the behavior of diaphragm-through joints of concrete-filled tubular columns”, *J. Mech. Mater. Struct.*, **7**(10), 909-929.

Sasaki, S., Teraoka, M., Morita, K. and Fujiwara, T. (1995), “Structural behavior of concrete-filled square tubular column with partial-penetration weld corner seam to steel H-beam connections”, *Proceeding of the 4th Pacific Structural Steel Conference*, Volume 2, pp. 33-40.

Yu, Y., Chen, Z. and Wang, X. (2015), “Effect of column flange flexibility on WF-beam to rectangular CFT column connections”, *J. Constr. Steel Res.*, **106**, 184-197.

Zhong, S.T. (2003), *The Concrete-Filled Steel Tubular Structures*, Tsinghua University Press, Beijing, China.

Zhou, T., Nie, S., Lu, L. and He, B. (2005), “Design of concrete-filled square tube column and steel beam joint with internal diaphragms”, *J. Build. Struct.*, **26**(5), 23-26.

CC